

# Quantum Hall effect induced by electron-phonon interaction

Andreas Sinner and Klaus Ziegler

*Institut für Physik, Universität Augsburg, D-86135 Augsburg, Germany*

When phonons couple to fermions in Weyl semimetals, the interaction may turn the system into an insulator. There are several phases the insulating state can be associated with, in particular a number of phases in which the time reversal and the sublattice symmetries are spontaneously broken. The examples are many body states commensurate to the Haldane staggered flux or to the modulated strain lattice models. We find that the effective field theories describing each of these phases exhibit the presence of phase specific topological terms. The coefficients of those generalized Chern-Simons terms are related to the topological invariants of microscopic model and hence to the quantized Hall conductivities with phase specific features.

PACS numbers: 05.60.Gg, 72.10.Bg, 73.22.Pr

*Introduction:* Upon a change of parameters a many-body Hamiltonian may describe a physical system passing through a transition between phases with very different properties. This process is usually accompanied by the symmetry change of ground states on both sides of the transition, the phenomenon known as the spontaneous symmetry breaking. The phase with the lower symmetry is characterized by the emergent macroscopic ordering of elementary building blocks of the system, technically captured by an order parameter. Phenomenological models describing the physics of the symmetry broken phase in terms of order parameters have proven very successful in description of various thermal and quantum phase transitions. In these models, critical parameters at which phase transitions occur correspond to emergent non-trivial potential minima and are approached using variational techniques, which lead to a set of mean-field equations for all order parameters. Sometimes, the ground states of a system is not uniquely determined by the order parameter alone, as they may have additional topological ordering [1, 2]. An important observation is that different phases of a degenerated ground state may be described by different topological field theories. Usually in condensed matter physics the emergence of the topological Chern-Simons excitations has not been considered in the broader context of symmetry breaking and phase transitions. To some extend only, is this the case for superfluid Helium, where  $^3\text{He} - \text{A}$  phase exhibits also a spontaneous time reversal symmetry breaking among other spontaneously broken symmetries [4–6].

The phase of the wave function can play a crucial role for the properties of the related physical system [7, 8]. In particular, if this phase is associated with a topological invariant through the winding number, it may describe robust macro-

scopic properties. Examples in condensed matter physics are the quantized Hall conductivity of electrons in 2d [1, 3, 10–13] and in quasi 1d structures [14]. Another example is the quantized transverse conductance of the supercurrent in the  $^3\text{He} - \text{A}$ -phase of superfluid liquid Helium [4–6], and quantized conductivities of different anomalous Hall effects [15–17]. In general, topological structures in 2+1-dimensional gauge field theories are related to Chern-Simons terms, where the coefficient in front of the latter is related to a topological invariant [18–21].

The properties of the tight-binding Hamiltonian describing the motion of electrons on the hexagonal lattice are well known and investigated in details in the existing literature [22, 23]. The Fourier transformed tight-binding Hamiltonian reads

$$H_{\text{TB}} = h_1(p)\sigma_1 + h_2(p)\sigma_2, \quad (1)$$

with  $h_1(p) = -t \sum_{i=1\dots 3} \cos(p \cdot a_i)$  and  $h_2(p) = -t \sum_{i=1\dots 3} \sin(p \cdot a_i)$ .  $t$  denotes the hopping amplitude,  $\sigma_i$  the Pauli matrices in usual representation, and  $\{a_i\}_{i=1,2,3}$  the vectors originating from the position of an atom on a sublattice of the hexagonal lattice to its nearest neighbors.  $H_{\text{TB}}$  is symmetric under time reversal

$$H_{\text{TB}}^*(-p) = H_{\text{TB}}(p), \quad (2)$$

where the complex conjugation acts only on the sublattice space. A spectral gap appears in the Hamiltonian in the form of the Dirac mass parameter  $m\sigma_3$  [23] and does not affect the property (2). The low-energy part of the spectrum is characterized by two Dirac cones at  $\mathbf{K}_{\pm}$ , which represent Fermi quasiparticles with different chiralities. They appear due to the bipartiteness of the hexagonal lattice and the reality of the hopping amplitude. One can find a representation in

which the effective Weyl Hamiltonian reads

$$H_0 = p_1 \Sigma_{01} + p_2 \Sigma_{32}, \quad (3)$$

where we employ the notation  $\Sigma_{ij} = \sigma_i \otimes \sigma_j$ ,  $i, j = 0, 1, 2, 3$ , with  $\sigma_i$  denoting the Pauli matrices. A reasonable translation of the property (2) into Weyl space is  $\Sigma_{02} H_0^T (-p) \Sigma_{02} = H_0(p)$  for the time reversal and  $\Sigma_{33} H_0 \Sigma_{33} = -H_0$  for the chiral or sublattice symmetry [24].

The simplest way to break the time reversal symmetry in tight-binding description is by attaching a complex phase to the hopping amplitudes between nearest neighbors. This so-called Peierls substitution trick is the common procedure for introducing gauge fields on the tight-binding lattices and is the basis for numerical studies of the integer quantum Hall effect [25]. Haldane found a way to avoid using homogeneous external magnetic field for breaking the time reversal symmetry by attaching the Peierls phase to the hopping amplitudes between second-nearest neighbors on the lattice [11, 26]. For different values of the Peierls phase one can realize a configuration with an alternating gap parameter, which changes its sign between both Dirac points. At a particular value of the Peierls phase  $\varphi = \pi/2$  the gap size at both cones is equally large but it has opposite signs. In the effective model this gap parameter couples to the  $\Sigma_{33}$  matrix. When added to the Weyl Hamiltonian, this term breaks both the time reversal and the sublattice symmetry and leads to a non-trivial topological response, known in the literature as the Hall effect without Landau levels [10, 11].

An entirely different gapped phase occurs in the modification of the tight-binding Hamiltonian with an applied modulated strain field. The gap parameter of this phase can be real valued and translationally invariant and couples to the matrix  $\Sigma_{12}$  on the Weyl space. This term breaks both discrete symmetries, too. An electron charge fractionalisation in a version of the Hamiltonian with modulated strain was reported in [27], which should have consequences for some observable quantities. An idea that dynamical lattice degrees of freedom can be treated as effective gauge fields is not new [28]. Here we study a system of monochromatic phonons minimally coupled to Weyl fermions. As the electron-phonon coupling strength increases the system should approach a transition into the structurally different phase. Our intention is to identify possible gapped phases, the corresponding quasiparticles and observables. A contact to the tight-binding models will help us to link these phases to different lattice distor-

tions, which lead to the formation of the spectral gaps with broken time reversal and sublattice symmetries. To emphasize the similarity of the phonons to the gauge fields we consider the  $E_1$ -optical phonon mode of a hexagonal lattice which represents individual vibrations of the sublattices in opposite directions [29, 30]. The number of modes is therefore naturally restricted to 2 and there is no time-like component of the effective gauge field. This resembles the popular in electrodynamics “light cone” gauge fixing  $\hat{n} \cdot \vec{A} = 0$ , with  $\hat{n}$  denoting a unit vector pointing into the time direction [2]. It was shown in [31] that in such system phonon Chern-Simons excitations can in principle be generated.

*Effective low-energy model:* Studying systems involving two Dirac fermions with different chiralities requires working in the space of  $4 \times 4$  complex matrices. In total there are 15 traceless matrices corresponding to a particular representation of the group of  $SU(4)$ -transformations and a 4-dimensional unit matrix  $\Sigma_{00}$ . For any complex  $4 \times 4$ -matrix  $\mathcal{Q}$  there is a unique decomposition  $\mathcal{Q} = \mathcal{Q}^{ij} \Sigma_{ij}$ . Assembling two particular subsets with two  $\Sigma$ -matrices each to vectors  $\vec{j} = \{\Sigma_{01}, \Sigma_{32}\}$  and  $\vec{\Pi} = \{\Sigma_{13}, \Sigma_{20}\}$  we introduce the effective low-energy model Hamiltonian as

$$\mathcal{H} = i \vec{\partial} \cdot \vec{j} + \vec{A} \cdot \vec{\Pi}, \quad (4)$$

where  $\vec{j}$  couples to the kinetic energy of fermions, while  $\vec{\Pi}$  to the two-component phonon field  $\vec{A}$ . In the lattice model the phonon field is attached to each bond while in low-energy approximation the phonon becomes local, is attached to each sublattice and accounts for the scattering between both Dirac nodes. The choice of the phonon part is not arbitrary though, but is dictated by the properties of the  $C_{6v}$  group [29, 32] and models the  $E_1$ -in-plane optical modes. The spectrum of these modes reveals a pronounced weak alteration over the entire Brillouin zone [30, 33, 34], which makes it possible to model them in the form of dispersionless monochromatic lattice vibrations. Neglecting the slow dynamics of heavy lattice ions we effectively end up with the following Euclidean action of an interacting electron-phonon system:

$$\mathcal{S}[A, \psi^\dagger, \psi] = \frac{1}{2g} \vec{A} \cdot \vec{A} + \psi^\dagger \cdot [\partial_\tau \Sigma_{00} + \mathcal{H}] \psi, \quad (5)$$

where  $\psi = (\psi_{11}, \psi_{12}, \psi_{21}, \psi_{22})^T$  denotes the 4-component Dirac bispinor with the first index referring to the sublattice and the second to the respective Dirac point. The coupling constant  $g$

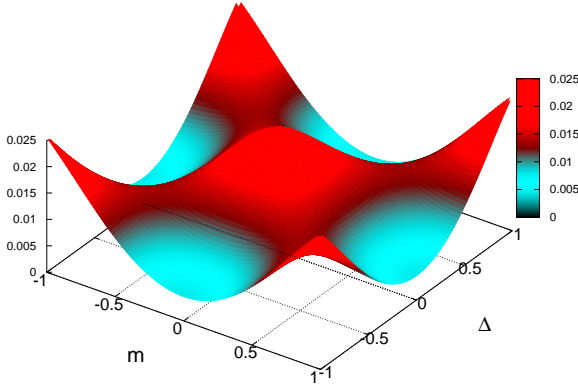


FIG. 1: Low-energy landscape of effective potential (11) with visible walls between stable phases. The model parameter are chosen to give  $\gamma = g/g_c \sim 3.5$ .

is related to the inverse frequency of monochromatic phonons [29, 31]. The correlation functions of currents can be obtained from the generating functional  $\mathcal{W}[\mathcal{A}] = \log\langle \exp\{-\mathcal{S}[\mathcal{A}]\} \rangle$  by repeating variations with respect to the fields  $\mathcal{A} = \{\vec{\alpha}, \vec{\beta}\}$ ,  $\mathcal{S}[\mathcal{A}]$  is the action (5) augmented by an auxiliary source term  $\psi^\dagger [\vec{\alpha} \cdot \vec{j} + \vec{\beta} \cdot \vec{\Pi}] \psi = \vec{\alpha} \cdot \vec{J}^{\text{intra}} + \vec{\beta} \cdot \vec{J}^{\text{inter}}$  with introduced intranodal and internodal current operators.  $\langle \dots \rangle$  denotes the functional integration over all degrees of freedom. Field  $\alpha$  is the external gauge field while field  $\beta$  could be an external mechanical modulated strain field. Particularly interesting for symmetry broken phases are non-vanishing average currents ( $\mu = 1, 2$ )

$$\bar{j}_{\mu,r}^{\text{intra}} = - \left. \frac{\delta}{\delta \alpha_{\mu,r}} \right|_{\mathcal{A}=0} \mathcal{W}[\mathcal{A}], \quad (6)$$

$$\bar{j}_{\mu,r}^{\text{inter}} = - \left. \frac{\delta}{\delta \beta_{\mu,r}} \right|_{\mathcal{A}=0} \mathcal{W}[\mathcal{A}]. \quad (7)$$

*Representation change and variational procedure:* Following the procedure developed in Ref. [32] we integrate the phonons  $A_\mu$ ,  $\mu = 1, 2$ , which creates a four-fermion interaction term. The latter can be decoupled anew by  $4 \times 4$  matrix fields  $\mathcal{Q}_\mu = \mathcal{Q}_\mu^{ij} \Sigma_{ij}$

$$\frac{g}{2} (\psi^\dagger \Pi_\mu \psi)^2 \rightarrow \frac{1}{2g} \text{tr} \mathcal{Q}_\mu^2 + i \psi^\dagger \mathcal{Q}_\mu \Pi_\mu \psi. \quad (8)$$

Integration over fermions yields a bosonic action

$$\mathcal{S}[\mathcal{Q}] = \frac{1}{2g} \text{tr} \mathcal{Q}_\mu^2 - \text{tr} \log [G_0^{-1} + i \mathcal{Q}_\mu \Pi_\mu], \quad (9)$$

where  $G_0^{-1} = \partial_\tau \Sigma_{00} + i \vec{\partial} \cdot \vec{j}$  is the inverse propagator of free Dirac electron.

In order to open a spectral gap, the mass parameter must couple to a matrix which does not commute with the Weyl Hamiltonian. Technically this prevents singularities on the real axis in the Green's functions. This requirement restricts our freedom to choose the order parameters to  $\mathcal{Q}_\mu \rightarrow \mathcal{Q}_\mu + M_\mu$ ,  $M_{1/2} = (\Delta \Sigma_{01/32} \pm m \Sigma_{20/13})/2$  with spatially uniform  $\Delta$  and  $m$ , such that

$$M = i M_\mu \Pi_\mu = m \Sigma_{33} + \Delta \Sigma_{12}, \quad (10)$$

which indeed anticommutes with  $H_0$  [35]. Inserting the order parameter matrix (10) into action (9) and neglecting fluctuations yields an effective potential in the symmetry broken phase

$$V_{\text{eff}} = \frac{1}{2g} \text{tr} M_\mu^2 - \log \det [G_0^{-1} + i M_\mu \Pi_\mu]. \quad (11)$$

The determinant can be readily evaluated giving for the second term  $-\int \frac{d^3 Q}{(2\pi)^3} \log [\Delta^4 + 2\Delta^2(Q^2 - m^2) + (Q^2 + m^2)^2]$ . The argument of the logarithm is not indifferent to the interchange of  $m$  and  $\Delta$ , which suggests the anisotropy of the potential. All integrals diverge and we need to perform the integrations up to a cutoff. The potential landscape plotted in Figure 1 reveals a high, yet discrete symmetry. Visually one observes four angular minima, corresponding to two stable phases with degenerated vacua separated from each other by potential walls. On the ridge of the potential one recognizes a fourfold degenerated saddle point like structure, which corresponds to the unstable states with strong tendency to decay in one of both stable phases. The  $\Delta$ - and the  $m$ -phase are associated with extra terms in the tight-binding Hamiltonian (1) in real space representation:

$$H_{\text{TB};\mathbf{r}\mathbf{r}'} + \Delta \sigma_2 \cos(\mathbf{G} \cdot \mathbf{r}) \delta_{\mathbf{r},\mathbf{r}'}, \quad (12)$$

where  $\mathbf{G} = \mathbf{K}_+ - \mathbf{K}_-$ , and

$$H_{\text{TB};\mathbf{r}\mathbf{r}'} + im\sigma_3 \sum_{j=1}^3 (\delta_{\mathbf{r}',\mathbf{r}+\mathbf{c}_j} - \delta_{\mathbf{r}',\mathbf{r}-\mathbf{c}_j}), \quad (13)$$

$\{\mathbf{c}_j\}_{j=1,2,3}$  denoting nearest neighbor basis vectors on one sublattice [11, 26]. The  $\Delta$ -phase is characterized by a strain field which modulates with the nodal wave vector  $\mathbf{G}$  (modulated strain phase), while the  $m$ -phase is a flux phase that is commensurate with one sublattice (Haldane phase). Both phases are subject to time reversal and sublattice symmetry breaking.

A more detailed picture is acquired from the solutions of mean field equations. They are obtained

if potential (11) is varied with respect to  $M_\alpha$ :

$$M_\alpha = ig\Pi_\alpha [G_0^{-1} + iM_\mu\Pi_\mu]_{rr}^{-1}. \quad (14)$$

Inserting the order parameter matrix in (14), performing the frequency integration from  $-\infty$  to  $+\infty$  and the radial integral up to the cutoff  $\Lambda$ , related to the band width we get

$$m \pm \Delta = \gamma(m \pm \Delta) \left[ \sqrt{1 + (m \pm \Delta)^2} - |m \pm \Delta| \right], \quad (15)$$

where  $\gamma = g\Lambda/2\pi$  and  $m$  and  $\Delta$  are rescaled in units of  $\Lambda$ . First we notice that  $m = \Delta$  might be a solution for both  $+$ , as well as trivially for  $-$  sign. This also includes  $m = 0 = \Delta$  case. Further solutions are there for  $m \neq 0, \Delta = 0$  or for  $m = 0, \Delta \neq 0$ . Generalizing we can extract non-trivial solutions from

$$1 = \gamma[\sqrt{1 + n^2\delta^2} - n|\delta|], \quad (16)$$

with  $n = 1$  for  $m \neq 0, \Delta = 0$  or for  $m = 0, \Delta \neq 0$  and  $n = 2$  if  $m = \Delta \neq 0$ , which gives a real solution only in the case if the interaction strength exceeds a critical value of the order of inverse band width  $\gamma = g/g_c \geq 1, g_c = 2\pi/\Lambda$

$$|\delta| = \frac{\gamma^2 - 1}{2n\gamma} \Theta(\gamma - 1). \quad (17)$$

The analysis of mean-field equations reveals two stable gapped phases with  $m$  and  $\Delta$  being the respective order parameters. The phase with  $m = \Delta$  is the unstable state of the model, c.f. Figure 1, and there are no any further real valued solutions.

*Gaussian term:* The Gaussian action is given by

$$\mathcal{S}_G[\mathcal{Q}] = \text{tr} \left\{ \frac{1}{2g} \mathcal{Q}_\mu^2 - \frac{1}{2} G \mathcal{Q}_\alpha \Pi_\alpha G \mathcal{Q}_\beta \Pi_\beta \right\}, \quad (18)$$

where  $G^{-1} = G_0^{-1} + M$  with the matrix  $M$  denoting the order parameter of the corresponding phase. Since fields  $\mathcal{Q}$  are  $4 \times 4$  matrices, the kernel (inverse phonon propagator matrix) of the quadratic form of Gaussian action is a  $32 \times 32$  matrix. Eq. (18) is analogous to

$$\mathcal{S}_G[\mathcal{Q}] = \vec{\mathcal{Q}}_r \cdot \mathcal{D}_{rr'}^{-1} \vec{\mathcal{Q}}_{r'}, \quad (19)$$

with the 32-dimensional real vector field  $\vec{\mathcal{Q}}$  assembled from the elements of the matrices  $\mathcal{Q}_{1,2}$  [32]. The stability of each phase follows from the positivity of the Proca matrices  $\mathcal{D}_{rr'}^{-1} \sim \mathbf{M}\delta_{rr'}$ . In accord with the intuitive picture drawn from the analysis of the effective potential, the Proca matrices of both  $m$ -phase and  $\Delta$ -phase are indeed

strictly positive, while in the mixed phase between them there are negative eigenvalues [36], rendering this phase unstable, see the discussion above.

*Generalized Chern-Simons terms:* The space of 16  $\Sigma$ -matrices subdivides into four sets of four matrices each, with three of them anticommuting among each other and the fourth commuting with all. Calling them  $A_{i=0 \dots 3}^{a=1 \dots 4}$ , imposing the normalization condition  $\text{Tr}[A_0^a A_1^a A_2^a A_3^a] = 4$  for all  $a$ , the sets become  $A^1 = \{i\Sigma_{00}, -\Sigma_{01}, -\Sigma_{32}, -\Sigma_{33}\}$ ,  $A^2 = \{-i\Sigma_{21}, \Sigma_{20}, -\Sigma_{13}, \Sigma_{12}\}$ ,  $A^3 = \{\Sigma_{30}, -i\Sigma_{31}, i\Sigma_{02}, -i\Sigma_{03}\}$ , and  $A^4 = \{-i\Sigma_{11}, \Sigma_{10}, \Sigma_{23}, -\Sigma_{22}\}$ . One recognizes that  $A^1$  and  $A^2$  are partially related to the vectors  $\vec{j}$  and  $\vec{\Pi}$  of the model defined in (4). Linear terms of gradient expansion of the action (18) in both phases can be brought into the form structurally similar to the Chern-Simons terms. The crucial difference is that rather than in terms of single components of  $\mathcal{Q}$ -fields, the Chern-Simons-like structure appears in terms of

$$\Lambda_i^a = \text{Tr}[A_i^a(\mathcal{Q}_\mu \Pi_\mu)] \quad (20)$$

for each set  $A^a$ . In  $m$ -phase linear terms resemble the conventional Chern-Simons terms, giving one Chern-Simons term for each set

$$\mathcal{S}_{CS}^m = S_m \epsilon_{ijk} \Lambda_i^a \cdot i\partial_j \Lambda_k^a, \quad (21)$$

where the dot-product implies the integration over the entire 3d space-time,  $i, j, k = 0, 1, 2$ , and  $S_m = \text{sgn}(m)/64\pi$ . The fact that in Eq. (21) derivatives with respect to spatial degrees of freedom appear alongside with the temporal suggests the maintenance of gauge invariance all through the calculations. The calculation of observable quantities requires both Proca and Chern-Simons terms. Because the Proca matrix has no zero eigenvalues the matrix  $\mathcal{D}^{-1}$  in (19) can be inverted even for zero momentum. For the  $\Delta$ -phase we get two morphologically different terms. The first one resembles the generalized multi-field Chern-Simons term

$$\mathcal{S}_{CS}^\Delta = S_\Delta \epsilon_{ijk} K_{ab} \Lambda_i^a \cdot i\partial_j \Lambda_k^b, \quad (22)$$

where upper indices run only over  $a, b = 1, 2$  and diagonal elements of symmetric tensor  $K$  are zero. Effectively it connects the intranodal and internodal currents with each other. The two remaining matrix sets  $A^3$  and  $A^4$  interact with each other in an unexpected way

$$\tilde{\mathcal{S}}_{CS}^\Delta = S_\Delta K_{ab} [\Lambda_3^a \cdot i\partial_i \Lambda_i^b - \Lambda_i^b \cdot i\partial_i \Lambda_3^a], \quad (23)$$

where  $i = 0, 1, 2$  and  $a, b = 3, 4$ . The two terms (22) and (23) are hardly discussed in context of induced Chern-Simons terms [12, 21].

*Generalized linear response:* Selecting only two Pauli sets  $\Lambda^1$  and  $\Lambda^2$  related to the effective model (4), we can combine both Eq. (21) and Eq. (22) for  $\alpha, \beta = 1, 2$  in one single expression

$$\mathcal{S}_{CS} = \epsilon_{ijk} T_{cd} \mathbf{\Lambda}_i^c \cdot i\partial_j \mathbf{\Lambda}_k^d, \quad (24)$$

where the diagonal elements of the symmetric tensor  $T_{cc} = \text{sgn}(m)/64\pi$  and non-diagonal ones  $T_{cd} = \text{sgn}(\Delta)/64\pi$ . This expression suggests the existence of the correlation function

$$\langle \mathbf{\Lambda}_{i,r}^c \mathbf{\Lambda}_{j,r'}^d \rangle_{\mathcal{G}} \sim T_{cd} i\epsilon_{ijk} \partial_k \delta(r - r'), \quad (25)$$

where  $\langle \dots \rangle_{\mathcal{G}}$  denotes the average with respect to the Gaussian weight (19). The evaluation of the functional integrals in Eq. (25) requires an explicit knowledge of elements of the Proca mass matrices in each phase. Some of elements of the Proca matrix sum up to multiples of  $\gamma^{-1}$  [36]. An important case is given with  $\mu, \nu = 1, 2$  and  $c, d = 1, 2$ , since it derives directly from the correlations of the currents (6) and (7)

$$\left. \frac{\delta}{\delta \mathcal{A}_{\nu,r'}^d} \frac{\delta}{\delta \mathcal{A}_{\mu,r}^c} \right|_{\mathcal{A}=0} \mathcal{W}[A] = \langle \mathbf{\Lambda}_{\mu,r}^c \mathbf{\Lambda}_{\nu,r'}^d \rangle_{\mathcal{G}}, \quad (26)$$

which enables us to define the generalized linear response formula

$$f_{\mu\nu}^{cd} = \int d^3r e^{-i\omega(\tau-\tau')} \langle \mathbf{\Lambda}_{\mu,r}^c \mathbf{\Lambda}_{\nu,r'}^d \rangle_{\mathcal{G}}. \quad (27)$$

For  $c = d = 1$  it is related to the usual Kubo conductivity formula via [32]

$$\sigma_{\mu\nu} = -\frac{\pi}{2\gamma^2} \lim_{\omega \rightarrow 0} \frac{f_{\mu\nu}^{11}}{\omega}. \quad (28)$$

Generalizing and performing the functional integration we find

$$-\frac{\pi}{2\gamma^2} \lim_{\omega \rightarrow 0} \frac{f_{\mu\nu}^{cd}}{\omega} = 64\pi T_{cd} \epsilon_{\mu\nu}. \quad (29)$$

Diagonal elements of (29) give the quantized response  $\text{sgn}(m)\epsilon_{\mu\nu}$  in the  $m$ -phase and the two off-diagonal components give the quantized response  $\text{sgn}(\Delta)\epsilon_{\mu\nu}$  of the  $\Delta$ -phase.  $c = d = 1$  corresponds to the usual intranodal Hall conductivity of two Dirac cones, while  $c = d = 2$  represents the average of two internodal currents, which gives the internodal Hall conductivity. The response in the  $\Delta$ -phase with  $c = 1, d = 2$  and vice versa represents the averages over products of an intra- and an internodal current flowing in perpendicular directions, which too has a quantized response.

*Discussions:* The low-energy behavior of free fermions on the hexagonal lattice is determined by separated spectral nodes. Because of these one can distinguish between currents directly linked to each node, i.e. the intranodal currents, and those between the nodes, i.e. the internodal currents. The system of such fermions coupled to the in-plane phonons can be formally interpreted as a gauge field theory. At sufficiently large electron-phonon interaction strength a transition into a structurally different lattice phase takes place, as visualized in Figure 1. We identify two distinct ground states with order parameters which break both the time reversal and the sublattice symmetries. The effective phonon model exhibits the Chern-Simons-like terms in both phases with coefficients related to quantized Hall conductivities. A similar effect of spontaneous time-reversal symmetry breaking was previously discussed for a time-periodic driven quantum system, where also a topological state with non-zero Chern numbers was observed [37]. This similarity indicates that the time-dependent phonon field plays the role of a time-periodic driving field.

For the experimental observation of the proposed effects we suggest the following setup: the measurement could be performed on a suspended tightened graphene sample which must be sufficiently flat in order to rule out disorder due to ripples and out-of-plane phonon modes. The in-plane phonon modes could be generated mechanically by applying modulated strain with variable frequency on the sample and by adjusting carefully the strain frequency to the energy of the  $E_1$ - mode. Estimations based on ab-initio calculations vary between 0.15–0.2eV [29, 34], which is well within the range of infrared Raman scattering technique [38]. In order to measure the Hall conductivities a weak electric gradient should be applied to the sample. In the case of the  $\Delta$ -phase, both electric and strain fields should be applied in the same direction to create the proposed quantized response.

## ACKNOWLEDGMENTS

We are grateful to Professor Aditi Mitra for drawing our attention to connections between time-periodically driven quantum systems and systems with electron-phonon interaction. This research was supported by the grants of the Julian Schwinger Foundation for Physics Research.

- 
- [1] E. Fradkin, *Field theories of condensed matter physics*, Cambridge University Press, Cambridge, UK (2013).
- [2] X. G. Wen, *Vacuum degeneracy of chiral spin states in compactified space*, Phys. Rev. B **40**, 7387(R) (1989).
- [3] D. J. Thouless, M. Kohmoto, M. P. Nightingale, and M. den Nijs, *Quantized Hall Conductance in a Two-Dimensional Periodic Potential*, Phys. Rev. Lett. **49**, 405 (1982).
- [4] G. E. Volovik, *Quantized Hall effect in superfluid Helium-3 film*, Phys. Lett. A **128**, 277 (1988).
- [5] G. E. Volovik, *An analog of the quantum Hall effect in a superfluid He<sup>3</sup> film*, Zh. Eksp. Teor. Fiz. **94**, 123 (1988) [Sov. Phys. JETP **67**, 1804 (1988)].
- [6] D. Vollhardt and P. Wölfle, *The Superfluid Phases of Helium 3*, Taylor & Francis, London, (1990).
- [7] Y. Aharonov and D. Bohm, *Significance of electromagnetic potentials in quantum theory*, Phys. Rev. **115**, 485 (1959).
- [8] M. V. Berry, *Quantal Phase Factors Accompanying Adiabatic Changes*, Proc. R. Soc. A **392**, 45 (1984).
- [9] B. I. Halperin, *Quantized Hall conductance, current-carrying edge states, and the existence of extended states in a two-dimensional disordered potential*, Phys. Rev. B **25**, 2185 (1982).
- [10] V. M. Yakovenko, *Chern-Simons terms and n field in Haldane's model for the quantum Hall effect without Landau levels*, Phys. Rev. Lett. **65**, 251 (1990).
- [11] F. D. M. Haldane, *Model for a quantum Hall effect without Landau levels: Condensed-matter realization of the "parity anomaly"*, Phys. Rev. Lett. **61**, 2015 (1988).
- [12] A. Zee, *Quantum hall fluids*, edited by H. B. Geyer *Field Theory, Topology and Condensed Matter Physics. Lecture Notes in Physics* (Springer, Berlin, Heidelberg, 1995), Vol **456**, 99–153.
- [13] J. Fröhlich and A. Zee, *Large scale physics of the quantum Hall fluid*, Nucl. Phys. B, **364**, 517 (1991).
- [14] H. Hettmansperger, F. Duerr, J. B. Oostinga, C. Gould, B. Trauzettel, and L. W. Molenkamp, *Quantum Hall effect in narrow graphene ribbons*, Phys. Rev. B **86**, 195417 (2012).
- [15] E. M. Hankiewicz, J. Li, T. Jungwirth, Q. Niu, S.-Q. Shen, and J. Sinova, *Charge Hall effect driven by spin-dependent chemical potential gradients and Onsager relations in mesoscopic systems*, Phys. Rev. B **72**, 155305 (2005).
- [16] P. Jacquod, R. S. Whitney, J. Meair, and M. Büttiker, *Onsager relations in coupled electric, thermoelectric, and spin transport: The tenfold way*, Phys. Rev. B **86**, 155118 (2012).
- [17] N. Nagaosa, J. Sinova, S. Onoda, A. H. MacDonald, and N. P. Ong, *Anomalous Hall effect*, Rev. Mod. Phys. **82**, 1539 (2010).
- [18] A. N. Redlich, *Parity violation and gauge noninvariance of the effective gauge field action in three dimensions*, Phys. Rev. D **29**, 2366 (1984).
- [19] R. Jackiw, *Fractional charge and zero modes for planar systems in a magnetic field*, Phys. Rev. D **29**, 2375 (1984).
- [20] E. Fradkin and F. Schaposnik, *The fermion-boson mapping in three-dimensional quantum field theory*, Phys. Lett. B **338**, 253 (1994).
- [21] G. Dunne, *Aspects of Chern-Simons theory*, in *Topological aspects of low dimensional systems*, edited by A. Comtet, T. Jolicœur, S. Ouvry, and F. David, Les Houches Summer School, (Springer, Berlin, Heidelberg, 1999), Vol. **69**, 177–263.
- [22] P. K. Wallace, *The band theory of graphite*, Phys. Rev. **71**, 622 (1947).
- [23] G. W. Semenoff, *Condensed-matter simulation of a three-dimensional anomaly*, Phys. Rev. Lett. **53**, 2449 (1984).
- [24] A.W.W. Ludwig, M.P.A. Fisher, R. Shankar, and G. Grinstein, *Integer quantum Hall transition: An alternative approach and exact results*, Phys. Rev. B **50**, 7526 (1994).
- [25] Y. Hatsugai and M. Kohmoto, *Energy spectrum and the quantum Hall effect on the square lattice with next-nearest-neighbor hopping*, Phys. Rev. B **42**, 8282 (1990).
- [26] A. Hill, A. Sinner and K. Ziegler, *Valley symmetry breaking and gap tuning in graphene by spin doping*, N. J. Ph. **13**, 035023 (2011).
- [27] C.-Y. Hou, C. Chamon, and C. Mudry, *Electron fractionalization in two-dimensional graphene like structures*, Phys. Rev. Lett. **98**, 186809 (2007).
- [28] E. Zohar, J. I. Cirac, and B. Reznik, *Quantum simulations of lattice gauge theories using ultracold atoms in optical lattices*, Rep. Prog. Phys. **79**, 014401 (2016).
- [29] D. M. Basko and I. L. Aleiner, *Interplay of Coulomb and electron-phonon interactions in graphene*, Phys. Rev. **77**, 041409(R) (2008).
- [30] B. Amorim, A. Cortijo, F. de Juan, A. G. Grushin, F. Guinea, A. Gutierrez-Rubio, H. Ochoa, V. Parante, R. Roldán, P. San-José, J. Schiefele, M. Sturla, M. A. H. Vozmediano, *Novel effects of strains in graphene and other two dimensional materials*, Phys. Rep. **617**, 1 (2016).
- [31] A. Sinner and K. Ziegler, *Emergent Chern-Simons excitations due to electron-phonon interaction*, Phys. Rev. B **93**, 125112 (2016).
- [32] A. Sinner and K. Ziegler, *Spontaneous mass generation due to phonons in a two-dimensional Dirac fermion system*, Ann. Phys. **400**, 262 (2019).
- [33] A. C. Ferrari, *Raman spectroscopy of graphene and graphite: Disorder, electron-phonon coupling, doping and nonadiabatic effects*, Sol. St. Comm. **143**, 47 (2007).
- [34] G. D. Sanders, A. R. T. Nugraha, K. Sato, J.-H. Kim, J. Kono, R. Saito and C. J. Stanton, *Theory of coherent phonons in carbon nanotubes and graphene nanoribbons*, J. Phys.: Condens. Matter **25**, 144201 (2013).
- [35] There are two further matrices which anticommute with  $H_0$ :  $\Sigma_{03}$  and  $\Sigma_{22}$ , but the mean-field

- solutions for respective order parameters are unstable. For  $\Sigma_{03}$  this is shown in Ref. [32], while the case of  $\Sigma_{22}$  is ruled out in the Supplement.
- [36] The elements of the Proca matrix and relations between them are given in the Supplement.
- [37] N.H. Lindner, G. Rafael, and V. Galitski, *Floquet topological insulator in semiconductor quantum wells*, Nature Phys. **7**, 490 (2011).
- [38] A. Jorio, *Raman Spectroscopy in Graphene-Based Systems: Prototypes for Nanoscience and Nanometrology*, ISRN Nanotechnology, Vol. **2012**, pp. 1-12 (2012).

## Supplement: Quantum Hall effect induced by electron-phonon interaction

Andreas Sinner and Klaus Ziegler  
*Institut für Physik, Universität Augsburg, D-86135 Augsburg, Germany*

### EXCLUSION OF $\Delta_2$ PARAMETER

Using the ansatz

$$M_1 = \frac{\Delta_1}{2}\Sigma_{01} - i\frac{\Delta_2}{2}\Sigma_{31} + \frac{m}{2}\Sigma_{20}, \quad M_2 = \frac{\Delta_1}{2}\Sigma_{32} - i\frac{\Delta_2}{2}\Sigma_{02} - \frac{m}{2}\Sigma_{13}, \quad (1)$$

with which

$$M = iM_\mu\Pi_\mu = m\Sigma_{33} + \Delta_1\Sigma_{12} + \Delta_2\Sigma_{22}. \quad (2)$$

we get to the set of mean-field equations

$$M_\alpha = ig\Pi_\alpha [G_0^{-1} + M]_{rr}^{-1}. \quad (3)$$

Projecting both sides on the subspaces of the composite order parameter we get for each  $\alpha$

$$m = \frac{g}{2}\text{Tr}\Sigma_{33} [G_0^{-1} + M]_{rr}^{-1}, \quad (4)$$

$$\Delta_1 = \frac{g}{2}\text{Tr}\Sigma_{12} [G_0^{-1} + M]_{rr}^{-1}, \quad (5)$$

$$\Delta_2 = -\frac{g}{2}\text{Tr}\Sigma_{22} [G_0^{-1} + M]_{rr}^{-1}, \quad (6)$$

which becomes after inverting the inverse propagator matrix

$$m = 2mg \int \frac{d^3Q}{(2\pi)^3} \frac{q_0^2 + q^2 + m^2 - \Delta_1^2 - \Delta_2^2}{m^4 + 2m^2(q_0^2 + q^2 - \Delta_1^2 - \Delta_2^2) + (q_0^2 + q^2 + \Delta_1^2 + \Delta_2^2)^2}, \quad (7)$$

$$\Delta_1 = 2\Delta_1g \int \frac{d^3Q}{(2\pi)^3} \frac{q_0^2 + q^2 - m^2 + \Delta_1^2 + \Delta_2^2}{m^4 + 2m^2(q_0^2 + q^2 - \Delta_1^2 - \Delta_2^2) + (q_0^2 + q^2 + \Delta_1^2 + \Delta_2^2)^2}, \quad (8)$$

$$\Delta_2 = -2\Delta_2g \int \frac{d^3Q}{(2\pi)^3} \frac{q_0^2 + q^2 - m^2 + \Delta_1^2 + \Delta_2^2}{m^4 + 2m^2(q_0^2 + q^2 - \Delta_1^2 - \Delta_2^2) + (q_0^2 + q^2 + \Delta_1^2 + \Delta_2^2)^2}. \quad (9)$$

If there are any mutually independent non-trivial solutions for  $\Delta_1$  and  $\Delta_2$  then they follow from

$$1 = 2g \int \frac{d^3Q}{(2\pi)^3} \frac{q_0^2 + q^2 - m^2 + \Delta_1^2 + \Delta_2^2}{m^4 + 2m^2(q_0^2 + q^2 - \Delta_1^2 - \Delta_2^2) + (q_0^2 + q^2 + \Delta_1^2 + \Delta_2^2)^2}, \quad (10)$$

$$1 = -2g \int \frac{d^3Q}{(2\pi)^3} \frac{q_0^2 + q^2 - m^2 + \Delta_1^2 + \Delta_2^2}{m^4 + 2m^2(q_0^2 + q^2 - \Delta_1^2 - \Delta_2^2) + (q_0^2 + q^2 + \Delta_1^2 + \Delta_2^2)^2}, \quad (11)$$

i. e. only one of them can be true and they cannot be fulfilled together. The two possibilities are

$$\Delta_1 = 0, \quad \Delta_2 \neq 0; \quad (12)$$

$$\Delta_2 = 0, \quad \Delta_1 \neq 0. \quad (13)$$

The scenario of Eq. (13) is discussed in the main text. Here we consider the scenario of Eq. (12), i. e.  $\Delta_1 = 0$  and  $\Delta_2 = \Delta$  is finite. The system of equations (7)-(9) reduces to

$$m = 2mg \int \frac{d^3Q}{(2\pi)^3} \frac{q_0^2 + q^2 + m^2 - \Delta^2}{m^4 + 2m^2(q_0^2 + q^2 - \Delta^2) + (q_0^2 + q^2 + \Delta^2)^2}, \quad (14)$$

$$\Delta = -2\Delta g \int \frac{d^3Q}{(2\pi)^3} \frac{q_0^2 + q^2 - m^2 + \Delta^2}{m^4 + 2m^2(q_0^2 + q^2 - \Delta^2) + (q_0^2 + q^2 + \Delta^2)^2}, \quad (15)$$

which upon integrating the frequency and angles becomes

$$m = \frac{g}{8\pi} \int_0^{\Lambda^2} dq^2 \left[ \frac{m - \Delta}{\sqrt{q^2 + (m - \Delta)^2}} + \frac{m + \Delta}{\sqrt{q^2 + (m + \Delta)^2}} \right], \quad (16)$$

$$\Delta = \frac{g}{8\pi} \int_0^{\Lambda^2} dq^2 \left[ \frac{m - \Delta}{\sqrt{q^2 + (m - \Delta)^2}} - \frac{m + \Delta}{\sqrt{q^2 + (m + \Delta)^2}} \right]. \quad (17)$$

Summing and subtracting them we get

$$m + \Delta = \frac{g}{4\pi} \int_0^{\Lambda^2} dq^2 \frac{m - \Delta}{\sqrt{q^2 + (m - \Delta)^2}}, \quad (18)$$

$$m - \Delta = \frac{g}{4\pi} \int_0^{\Lambda^2} dq^2 \frac{m + \Delta}{\sqrt{q^2 + (m + \Delta)^2}}. \quad (19)$$

While the limit  $\Delta = 0$ ,  $m \neq 0$  is well defined, another limit  $m = 0$ ,  $\Delta \neq 0$  is not (left hand side is negative, right hand side is positive) which suggests that the  $\Delta$ -phase cannot exist alone. It remains to check the case of coexistence of both parameters, which arises as the solution of

$$m \pm \Delta = \gamma(m \mp \Delta) \left[ \sqrt{1 + (m \mp \Delta)^2} - |m \mp \Delta| \right], \quad (20)$$

which appears after integrating the momenta and rescaling all quantities as  $m \rightarrow \Lambda m$ ,  $\Delta \rightarrow \Lambda \Delta$ ,  $\gamma = g\Lambda/2\pi$ . The expression in the squared brackets is positive, i. e. the full equation has any sense only if the sign of  $m \pm \Delta$  and  $m \mp \Delta$  are the same, which for positive  $m$  and  $\Delta$  suggests  $|m| > |\Delta|$ . Below we assume both sides to be positive. Rewriting it as

$$\frac{m \pm \Delta}{\gamma} + (m \mp \Delta)^2 = (m \mp \Delta) \sqrt{1 + (m \mp \Delta)^2}, \quad (21)$$

and squaring both sides we get

$$\frac{1}{\gamma^2} (m \pm \Delta)^2 = (m \mp \Delta)^2 \left[ 1 - \frac{2}{\gamma} (m \pm \Delta) \right]. \quad (22)$$

Separating terms which are unique in the sign from those appearing with  $\pm$  we find

$$\frac{m^2 + \Delta^2}{\gamma^2} - \left( 1 - \frac{2m}{\gamma} \right) (m^2 + \Delta^2) - \frac{4m\Delta^2}{\gamma^2} = \mp \frac{2\Delta}{\gamma} \left( \frac{m}{\gamma} + m^2 + \Delta^2 + \gamma m \left( 1 - 2\frac{m}{\gamma} \right) \right), \quad (23)$$

which can only make sense if both sides vanish individually. Left hand side yields

$$\Delta^2 = -m^2 \frac{1 - \gamma^2 + 2\gamma m}{1 - \gamma^2 - 2\gamma m}, \quad (24)$$

while right hand side gives

$$\Delta^2 = -\frac{m}{\gamma} [1 + \gamma^2 - m\gamma]. \quad (25)$$

Equating both right hand sides yields

$$|m| = \frac{1 - \gamma^4}{4\gamma}, \quad (26)$$

i. e. it is semi-positive if  $\gamma \leq 1$  and predicts a non-physical phase for small  $\gamma$ . Moreover, plugging it back yields for  $\Delta$

$$\Delta^2 = -\frac{1 - \gamma^4}{16\gamma^2} [\gamma^4 + 4\gamma^2 + 3], \quad (27)$$

which is negative for  $\gamma \leq 1$ . But this means that  $\Delta$  is imaginary which conflicts with the requirement for the effective Hamiltonian to be hermitian. Hence the order parameter  $\Delta_2$  must be excluded from the further consideration.

### STRUCTURE OF THE PROCA TERM

The Gaussian action is defined by Eq. (19) in the main part

$$\mathcal{S}_G[\mathcal{Q}] = \vec{\mathcal{Q}}_r \cdot \mathcal{D}_{rr'}^{-1} \vec{\mathcal{Q}}_{r'}, \quad (28)$$

where the real vector field  $\vec{\mathcal{Q}}_r = (\vec{\mathcal{Q}}_1, \vec{\mathcal{Q}}_2)_r^\top$

$$\vec{\mathcal{Q}}_i = (\mathcal{Q}_i^{00}, \mathcal{Q}_i^{01}, \mathcal{Q}_i^{02}, \mathcal{Q}_i^{03}, \mathcal{Q}_i^{10}, \mathcal{Q}_i^{11}, \mathcal{Q}_i^{12}, \mathcal{Q}_i^{13}, \mathcal{Q}_i^{20}, \mathcal{Q}_i^{21}, \mathcal{Q}_i^{22}, \mathcal{Q}_i^{23}, \mathcal{Q}_i^{30}, \mathcal{Q}_i^{31}, \mathcal{Q}_i^{32}, \mathcal{Q}_i^{33}), \quad i = 1, 2. \quad (29)$$

The matrix  $\mathcal{D}_{rr'}^{-1}$  is different for each phase. Below we give Proca matrices for all phases.

1.  $m$ -phase:

$$\begin{aligned} \mathcal{D}_{Q=0}^{-1} = & M_1 (e_{1,1} + e_{4,4} + e_{10,10} + e_{11,11} + e_{17,17} + e_{20,20} + e_{26,26} + e_{27,27}) \\ & + M_2 (e_{2,2} + e_{9,9} + e_{24,24} + e_{31,31}) \\ & + M_3 (e_{3,3} + e_{8,8} + e_{12,12} + e_{15,15} + e_{18,18} + e_{21,21} + e_{25,25} + e_{30,30}) \\ & + M_4 (e_{5,5} + e_{14,14} + e_{19,19} + e_{28,28}) \\ & + M_5 (e_{6,6} + e_{7,7} + e_{13,13} + e_{16,16} + e_{22,22} + e_{23,23} + e_{29,29} + e_{32,32}) \\ & - iD_1 (e_{1,32} + e_{4,29} + e_{6,27} - e_{7,26} + e_{10,23} - e_{11,22} - e_{13,20} - e_{16,17} \\ & - e_{17,16} - e_{20,13} - e_{22,11} + e_{23,10} - e_{26,7} + e_{27,6} + e_{29,4} + e_{32,1}) \\ & - D_2 (e_{2,31} - e_{5,28} - e_{9,24} - e_{14,19} - e_{19,14} - e_{24,9} - e_{28,5} + e_{31,2}). \end{aligned}$$

Explicitly, the matrix elements are

$$\begin{aligned} M_1 &= \frac{2}{\gamma} + \frac{1}{2\sqrt{1+m^2}}, & M_2 &= \frac{2}{\gamma} + 2m - \frac{1+2m^2}{\sqrt{1+m^2}}, & M_3 &= \frac{2}{\gamma}, \\ M_4 &= \frac{2}{\gamma} - 2m + \frac{1+2m^2}{\sqrt{1+m^2}}, & M_5 &= \frac{2}{\gamma} - \frac{1}{2\sqrt{1+m^2}}, \\ D_1 &= \frac{1}{2\sqrt{1+m^2}}, & D_2 &= -2m + \frac{1+2m^2}{2\sqrt{1+m^2}}. \end{aligned} \quad (30)$$

The difference in comparison to representation in Ref. [1] is explained by the fact that some of the matrix elements given there happen to vanish by integration. The matrix elements fulfill following equalities:

$$M_1 + M_5 = \frac{4}{\gamma}, \quad M_1 - D_1 = \frac{2}{\gamma} = M_5 + D_1 \quad (31)$$

$$M_2 + M_4 = \frac{4}{\gamma}, \quad M_2 + D_2 = \frac{2}{\gamma} = M_4 - D_2. \quad (32)$$

The eigenvalues of the Gauss matrix for this case are

$$E_{1\dots 28}^m = \frac{2}{\gamma}, \quad E_{29,30}^m = \frac{2(3+\gamma^2)}{\gamma+\gamma^3}, \quad E_{31,32}^m = \frac{2(\gamma^2-1)}{\gamma+\gamma^3}. \quad (33)$$

2.  $\Delta$ -phase:

$$\begin{aligned} \mathcal{D}_{Q=0}^{-1} = & M_1 (e_{1,1} + e_{10,10} + e_{17,17} + e_{26,26}) + M_2 (e_{2,2} + e_{9,9} + e_{24,24} + e_{31,31}) \\ & + M_3 (e_{3,3} + e_{12,12} + e_{21,21} + e_{30,30}) + M_4 (e_{4,4} + e_{11,11} + e_{20,20} + e_{27,27}) \\ & + M_5 (e_{5,5} + e_{14,14} + e_{19,19} + e_{28,28}) + M_6 (e_{6,6} + e_{13,13} + e_{22,22} + e_{29,29}) \\ & + M_7 (e_{7,7} + e_{16,16} + e_{23,23} + e_{32,32}) + M_8 (e_{8,8} + e_{15,15} + e_{18,18} + e_{25,25}) \\ & + iD_1 (e_{1,32} - e_{7,26} + e_{10,23} - e_{16,17} - e_{17,16} + e_{23,10} - e_{26,7} + e_{32,1}) \\ & + D_2 (e_{2,31} - e_{9,24} - e_{24,9} + e_{31,2}) + D_3 (e_{3,30} + e_{12,21} + e_{21,12} + e_{30,3}) \\ & - iD_4 (e_{4,29} + e_{6,27} - e_{11,22} - e_{13,20} - e_{20,13} - e_{22,11} + e_{27,6} + e_{29,4}) \\ & + D_5 (e_{5,28} + e_{14,19} + e_{19,14} + e_{28,5}). \end{aligned}$$

The matrix elements are

$$\begin{aligned}
M_1 &= \frac{2}{\gamma} + \frac{1}{2\sqrt{1+\Delta^2}}, & M_2 &= \frac{2}{\gamma} + 2\Delta - \frac{1+2\Delta^2}{\sqrt{1+\Delta^2}}, & M_3 &= \frac{2}{\gamma} - \Delta + \frac{\Delta^2}{\sqrt{1+\Delta^2}}, \\
M_4 &= \frac{2}{\gamma} - \Delta + \frac{1+2\Delta^2}{2\sqrt{1+\Delta^2}}, & M_5 &= \frac{2}{\gamma} - \Delta + \sqrt{1+\Delta^2}, & M_6 &= \frac{2}{\gamma} + \Delta - \frac{1+2\Delta^2}{2\sqrt{1+\Delta^2}}, \\
M_7 &= \frac{2}{\gamma} - \frac{1}{2\sqrt{1+\Delta^2}}, & M_8 &= \frac{2}{\gamma}, \\
D_1 &= -\frac{1}{2\sqrt{1+\Delta^2}}, & D_2 &= 2\Delta - \frac{1+2\Delta^2}{2\sqrt{1+\Delta^2}}, & D_3 &= \Delta - \frac{\Delta^2}{\sqrt{1+\Delta^2}}, \\
D_4 &= -\Delta + \frac{1+2\Delta^2}{2\sqrt{1+\Delta^2}}, & D_5 &= \sqrt{1+\Delta^2} - \Delta,
\end{aligned} \tag{34}$$

We notice following most important equalities which are fulfilled by the matrix elements:

$$M_1 + M_7 = \frac{4}{\gamma}, \quad M_1 + D_1 = \frac{2}{\gamma} = M_7 - D_1 \tag{35}$$

$$M_4 + M_6 = \frac{4}{\gamma}, \quad M_2 - D_2 = \frac{2}{\gamma} = M_4 - D_4. \tag{36}$$

The stability matrix has the following eigenvalues :

$$E_{1\dots 26}^\Delta = \frac{2}{\gamma}, \quad E_{27,28}^\Delta = \frac{4}{\gamma}, \quad E_{29,30}^\Delta = \frac{4}{\gamma + \gamma^3}, \quad E_{31,32}^\Delta = \frac{2(\gamma^2 - 1)}{\gamma + \gamma^3}. \tag{37}$$

Last two eigenvalues are related to the order parameter of the phase  $\Delta$  in Eq. (17) in the main part.

### 3. Coexisting phase $m = \Delta$ :

$$\begin{aligned}
\mathcal{D}^{-1} &= M_1 (e_{1,1} + e_{10,10} + e_{17,17} + e_{26,26}) + M_2 (e_{2,2} + e_{9,9} + e_{24,24} + e_{31,31}) \\
&+ M_3 (e_{3,3} + e_{12,12} + e_{21,21} + e_{30,30}) + M_4 (e_{4,4} + e_{11,11} + e_{20,20} + e_{27,27}) \\
&+ M_5 (e_{5,5} + e_{14,14} + e_{19,19} + e_{28,28}) + M_6 (e_{6,6} + e_{13,13} + e_{22,22} + e_{29,29}) \\
&+ M_7 (e_{7,7} + e_{16,16} + e_{23,23} + e_{32,32}) + M_8 (e_{8,8} + e_{15,15} + e_{18,18} + e_{25,25}) \\
&+ A_1 (e_{1,10} - e_{7,16} + e_{10,1} - e_{16,7} - ie_{1,23} + ie_{7,17} - ie_{10,32} + ie_{16,26} \\
&+ ie_{17,7} - ie_{23,1} + ie_{26,16} - ie_{32,10} + e_{17,26} - e_{23,32} + e_{26,17} - e_{32,23}) \\
&+ A_2 (e_{2,9} + e_{9,2} - e_{2,24} + e_{9,31} - e_{24,2} + e_{31,9} - e_{24,31} - e_{31,24}) \\
&+ A_3 (e_{3,30} + e_{12,21} + e_{21,12} + e_{30,3}) \\
&+ iD_1 (e_{1,32} - e_{7,26} + e_{10,23} - e_{16,17} - e_{17,16} + e_{23,10} - e_{26,7} + e_{32,1}) \\
&+ D_2 (e_{2,31} - e_{9,24} - e_{24,9} + e_{31,2}) \\
&- iD_3 (e_{4,29} + e_{6,27} - e_{11,22} - e_{13,20} - e_{20,13} - e_{22,11} + e_{27,6} + e_{29,4}) \\
&+ D_4 (e_{5,28} + e_{14,19} + e_{19,14} + e_{28,5}).
\end{aligned}$$

Each quantity in the Proca matrix means

$$\begin{aligned}
A_1 &= \frac{1 - \sqrt{1+4m^2}}{4\sqrt{1+4m^2}}, \\
A_2 &= \frac{1}{2} \left[ 1 + 4m - 2\sqrt{1+4m^2} + \frac{1}{\sqrt{1+4m^2}} \right], \\
A_3 &= -\frac{1}{6m^2} \left[ 1 - \sqrt{1+4m^2} + 2m^2 \left( \sqrt{1+4m^2} - 2m \right) \right].
\end{aligned}$$

Matrix elements  $A_{1\dots 3}$  appear only as consequence of coexisting order parameters  $m$  and  $\Delta$ .

$$\begin{aligned}
M_1 &= \frac{2}{\gamma} + \frac{1 + \sqrt{1 + 4m^2}}{4\sqrt{1 + 4m^2}}, \\
M_2 &= \frac{2}{\gamma} + \frac{1}{2} \left[ 4m - 1 - 2\sqrt{1 + 4m^2} + \frac{1}{\sqrt{1 + 4m^2}} \right], \\
M_3 &= \frac{2}{\gamma} + \frac{1}{6m^2} \left[ 1 - \sqrt{1 + 4m^2} + 2m^2 \left( \sqrt{1 + 4m^2} - 2m \right) \right], \\
M_4 &= \frac{2}{\gamma} - \frac{1}{12m^2} \left[ 1 - \sqrt{1 + 4m^2} - 4m^2 \left( \sqrt{1 + 4m^2} - 2m \right) \right], \\
M_5 &= \frac{2}{\gamma} - 2m + \sqrt{1 + 4m^2}, \\
M_6 &= \frac{2}{\gamma} + \frac{1}{12m^2} \left[ 1 - \sqrt{1 + 4m^2} - 4m^2 \left( \sqrt{1 + 4m^2} - 2m \right) \right], \\
M_7 &= \frac{2}{\gamma} - \frac{1 + \sqrt{1 + 4m^2}}{4\sqrt{1 + 4m^2}}, \\
M_8 &= \frac{2}{\gamma}.
\end{aligned}$$

where (and further on)  $m$  is defined in Eq. (17) in the main part.

$$\begin{aligned}
D_1 &= -\frac{1 + \sqrt{1 + 4m^2}}{4\sqrt{1 + 4m^2}}, \\
D_2 &= \frac{1}{2} \left[ 4m - 1 - 2\sqrt{1 + 4m^2} + \frac{1}{\sqrt{1 + 4m^2}} \right], \\
D_3 &= -\frac{1}{12m^2} \left[ 1 - \sqrt{1 + 4m^2} - 4m^2 \left( \sqrt{1 + 4m^2} - 2m \right) \right], \\
D_4 &= \sqrt{1 + 4m^2} - 2m.
\end{aligned}$$

The stability matrix has following eigenvalues

$$E_{1\dots 26} = \frac{2}{\gamma}, \quad E_{27,28} = \frac{4}{\gamma}, \quad E_{29,30} = \frac{8}{3\gamma} \frac{1 + 2\gamma}{(1 + \gamma)^2}, \quad E_{31} = \frac{2(\gamma^2 - 1)}{\gamma + \gamma^3} \quad (38)$$

the latter related to the order parameter defined in Eq. (17) in the main text. However, the last remaining eigenvalue

$$E_{32} = -2 + \frac{2}{\gamma} \quad (39)$$

is negative for all  $\gamma > 1$ .

---

[1] A. Sinner and K. Ziegler, *Spontaneous mass generation due to phonons in a two-dimensional Dirac fermion system*, Ann. Phys. **400**, 262 (2019).